A novel microbial-derived family 19 endochitinase with exochitinase activity and its immobilization

Aijia Xing[1,2] · Yang Hu[1,2] · Wei Wang[1,2] · Francesco Secundo[3] · Changhu Xue[1,2,4] · Xiangzhao Mao[1,2,4]

Abstract

A novel chitinase gene of 888 bp from *Streptomyces bacillaris* was cloned and expressed in *Escherichia coli* BL21. The purified recombinant enzyme (SbChiAJ103) was identified as the first microbial-derived family 19 endochitinase that showed exochitinase activity. SbChiAJ103 exhibited the substrate preference for *N*-acetylchitooligosaccharides with even degrees of polymerization and the capability to specifically hydrolyze colloidal chitin into $(GlcNAc)_2$. Mono-methyl adipate was employed as a novel linker for the efficient covalent immobilization of chitinase on magnetic nanoparticles (MNPs). The immobilized SbChiAJ103, SbChiAJ103@MNPs, exhibited superior pH tolerance, temperature stability, and storage stability than free SbChiAJ103. Even after incubation at 45 °C for 24 h, SbChiAJ103@MNPs could retain more than 60.0% initial activity. As a result, the enzymatic hydrolysis yield of SbChiAJ103@MNPs increased to 1.58 times that of free SbChiAJ103. Moreover, SbChiAJ103@MNPs could be reused by convenient magnetic separation. After 10 recycles, SbChiAJ103@MNPs could retain almost 80.0% of its initial activity. The immobilization of the novel chitinase SbChiAJ103 paves the way to the efficient and eco-friendly commercial production of $(GlcNAc)_2$.

Key points

● *The first microbial GH19 endochitinase with exochitinase activity was reported.*
● *Mono-methyl adipate was first employed to immobilize chitinase.*
● *SbChiAJ103@MNPs showed excellent pH stability, thermal stability, and reusability.*

Keywords Chitinase · Immobilization · Magnetic nanoparticles · Chitin · *N*-acetylchitooligosaccharides

Introduction

N-acetylchitooligosaccharides (NCOS) have been widely used in the fields of food, cosmetics, agriculture, and medicine, due to their low-calorie property, moisturizing capability, and antibacterial, antiinflammatory, and antitumor activities (Chen et al.

✉ Yang Hu
  huyang@ouc.edu.cn

1 Qingdao Key Laboratory of Food Biotechnology, College of Food Science and Engineering, Ocean University of China, Qingdao 266003, China

2 Key Laboratory of Biological Processing of Aquatic Products, China National Light Industry, Qingdao, China

3 Istituto di Scienze e Tecnologie Chimiche "Giulio Natta", CNR, v. Mario Bianco 9, 20131 Milan, Italy

4 Laboratory for Marine Drugs and Bioproducts of Qingdao, National Laboratory for Marine Science and Technology, Qingdao 266237, China

2010; Ngo et al. 2008). As the degradation products of chitin, NCOS can be produced by chemical, physical, and enzymatic methods. The enzymatic hydrolysis of chitin is considered as an environmentally friendly, efficient, and convenient method for the preparation of value-added NCOS (Mao et al. 2017). Chitinase with high catalytic performance is the most widely used enzyme in the enzymatic preparation of NCOS. The specificity of chitinase allows it to produce oligosaccharides with a single polymerization degree from chitin. For example, chitinase was reported to efficiently prepare *N,N´*-diacetylchitobiose [(GlcNAc)₂] (Yang et al. 2016a, b). By virtue of the high specificity and catalytic efficiency, chitinases have been used to treat chitin from marine waste and purify oligosaccharide products for the industrial preparation of NCOS (Doan et al. 2021).

According to the amino acid sequence homology and protein structure, chitinases can be mainly categorized into glycoside hydrolases family 18 (GH18) and family 19 (GH19) (Cantarel et al. 2009). In addition, chitinases belonging to family 23 (GH23) and family 48 (GH48) have also been recently discovered separately in *Pyrococcus chitonophagus*

and the active adults of the leaf beetle *Gastrophysa atro-cyanea* (Nishitani et al. 2018; Fujita et al. 2006). It has been reported that GH18 chitinases widely exist in kinds of organisms, while most of the GH19 chitinases are from plants (Chen et al. 2020; Hoell et al. 2006). Also, the reported GH19 chitinases were found to originate from *Streptomyces*, such as *S. alfalfae* (Lv et al. 2021), *S. sampsonii* (Zhang et al. 2020), *S. griseus* (Hoster et al. 2005; Watanabe et al. 1999), *S. cyaneus* (Yano et al. 2008), *S. coelicolor* (Kawase et al. 2006), and *S. venezuelae* (Mukherjee and Sen 2006). These chitinases show molecular weights of approximately 30 kDa with the optimum temperature range from 45 to 60 °C. Although the optimum pH values of the existing GH19 chitinases range from 4.5 to 8.0, their activities were not high enough in a neutral environment at the reaction temperature below 50 °C, with room to be improved for meeting the requirement of industrial production of NCOS. Therefore, the research of a new chitinase with high enzyme activity and catalytic efficiency under a neutral condition at relatively low temperature is necessary for the enzymatic preparation of NCOS.

Free chitinases are sensitive to the environment and difficult to recover, which is another factor limiting their application in the industrial NCOS production. The enzyme immobilization technique can improve enzyme stability and allow the biocatalyst reused, thereby improving the utilization of enzyme (Ricardi et al. 2021). Common carriers for enzyme immobilization include natural polymers, composite polymers, and nanomaterials. Among them, nanomaterials are considered as outstanding carriers due to their large specific surface area and good dispersity. Therefore, enzyme immobilization based on nanomaterials usually displays high enzyme load and mobility, beneficial for the enzymatic catalysis (Wang et al. 2015). In particular, magnetic nanomaterials that could be conveniently recovered from reaction solutions by magnetic separation have been widely used as the carriers for enzyme immobilization (Lei et al. 2011). A firm connection between enzyme and magnetic carrier is required to reduce enzyme leakage and improve enzyme stability (Ein Ali Afjeh et al. 2020). Commonly, the covalent method using glutaraldehyde as the cross-linking agent is employed for covalent enzyme immobilization (Kidibule et al. 2021). However, glutaraldehyde-based immobilization generally decreased the activity of immobilized enzymes (Barbosa et al. 2014). Besides, the potential toxicity of glutaraldehyde brings the problem of biological incompatibility to immobilized chitinase, which limits the application of immobilized chitinase in the production of high-value NCOS (Zheng et al. 2022). In our previous studies, 2,4,6-trichloro-1,3,5-triazine was used as linker to improve the stability and reusability of immobilized chitosanase on magnetite nanoparticles (Wang et al. 2018). However, the low cross-linking efficiency of 2,4,6-trichloro-1,3,5-triazine

resulted in a relative low enzyme loading, which needs to be further improved to meet the needs of industrial production. Therefore, a biocompatible efficient cross-linking agent that has few adverse effects on the activity of immobilized chitinase is required to prepare the high-efficiency immobilized chitinase for NCOS production.

In this study, a novel chitinase SbChiAJ103 from *S. bacillaris* was cloned and expressed for the enzymatic production of NCOS. The enzymatic properties and hydrolysis patterns of SbChiAJ103 were investigated. With the aim to improve the stability and realize the reusability of the chitinase, biocompatible mono-methyl adipate (MMA) was used as the linker to functionalize the magnetic nanoparticles for the immobilization of SbChiAJ103. The morphology and magnetism of the prepared magnetic nanoparticles were characterized. Then, the enzymatic properties of immobilized chitinase were extensively investigated in the terms of thermal stability, pH stability, reusability, and enzymatic hydrolysis yield. The results obtained in the research are expected to be a reliable way for the industrial production of NCOS.

Materials and methods

Materials and reagents

Chitin was obtained from Yuanye Biotech (Shanghai, China) and used to prepare colloidal chitin in enzymatic activity measurements, according to the method from Gao et al. (Gao et al. 2018). The Rapid Mini plasmid kit was purchased from TianGen Biotech (Beijing, China). The DNA polymerase was obtained from Toyobo (Osaka, Japan). Ni–NTA resin was from TransGen Biotech (Beijing, China). 3,5-dinitrosalicylic acid (DNS) was obtained by Solarbio Co. (Beijing, China). NCOS with 2–6 degrees of polymerization (DP) were obtained from BZ Oligo Biotech (Qingdao, China). Ammonium hydroxide ($NH_3 \cdot H_2O$), ferrous chloride ($FeCl_2$), ferric chloride hexahydrate ($FeCl_3 \cdot 6H_2O$), 1-(3-dimethylaminopropyl)-3-ethylcarbodiimide hydrochloride (EDC), 4-morpholine ethane sulfonic (MES), *N*-hydroxysuccinimide (NHS), mono-methyl adipate (MMA), and lithium hydroxide (LiOH) were purchased from Macklin Co. (Shanghai, China). Tetraethyl orthosilicate (TEOS) was purchased from Sinopharm Group Co. Ltd. (Shanghai, China). Amino propyl tri-ethoxi silane (APTES) was obtained from Sigma Co. (Houston, TX, USA). All other reagents were of analytical grade obtained from local suppliers.

Gene cloning and sequence analysis of SbChiAJ103

The bacterial strain, *Streptomyces bacillaris* ATCC 15,855, was obtained from China General Microbiological Culture Collection Center (CGMCC 4.1584). Using the genomic

DNA of *S. bacillaris* ATCC 15,855 as the template, the chitinase gene *SbChiAJ103* was amplified through polymerase chain reaction (PCR) with two primers, (5′-GCGGCCGCA AGCTTGCAGCTCAGGTTGG-3′) and (5′-CAAATGGGT CGCGGATCCATGGTGTTCAAACGTG-3′) from Sangon Biotech. The PCR reaction was programmed as below: predegeneration at 95 °C for 10 min, amplification of 30 cycles (98 °C for 10 s, 64 °C for 30 s, 68 °C for 1 min), and a final extension for 10 min at 68 °C. The gene sequences from NCBI and CAZy databases were used to construct the evolutionary tree by MEGA 6.0 (Tamura et al. 2013). The phylogenetic tree was constructed using the neighbor-joining (NJ) method. The functional structure domains of SbChiAJ103 were predicted by the Simple Modular Architecture Research Tool (SMART) (Schultz et al. 2000). Protein homologous sequence alignment was performed by ClustalW to identify conserved residues (Jeffrey Yuan 1999).

Expression and purification of SbChiAJ103

The recombinant plasmid pET28a-SbChiAJ103 that contained the chitinase gene *SbChiAJ103* and a 6×His C-term tag was built and transformed into *E. coli* BL21 (DE3). In this process, 10 µL of recombinant plasmid was added to 100 µL of *E. coli* BL21 competent cells and sequentially placed on ice for 30 min, 42 °C for 45 s, and ice bath for 2 min. Then, 700 µL of medium without antibiotics was added for recovery at 37 °C for 1 h. A single colony that harbored the recombinant plasmid was picked and inoculated to a ZYP-5052 autoinduction medium at 20 °C for 48 h with a rotation speed of 220 rpm for the expression of chitinase SbChiAJ103. Then, the cells were collected by centrifugation and resuspended in a lysis buffer (50 mM Tris–HCl, pH 8.0). Subsequently, the suspension was treated with ultrasonication to extract chitinase SbChiAJ103. After refrigerated centrifugation (8000 rpm, 4 °C, 20 min), the supernatant containing crude enzyme was collected and loaded onto a Ni–NTA column (20×100 mm) for purification. The binding buffer (10 mM imidazole solution), wash buffers (20 mM and 40 mM imidazole solution), and elution buffer (60 mM imidazole solution) were employed in the purification process of SbChiAJ103. Finally, the purified protein was analyzed by sodium dodecyl sulfate polyacrylamide gel electrophoresis (SDS-PAGE).

Enzyme activity and enzymatic hydrolysis products assay

The activity of SbChiAJ103 was evaluated by the hydrolysis of colloidal chitin, according to the method from Gao et al. (Gao et al. 2018). Ten microliters of the purified enzyme was added to 190 µL (1.0% w/v) colloidal chitin solution (pH 7.0 sodium phosphate buffer) and reacted at 45 °C for 30 min. Then, the reaction was stopped by boiling water bath for 10 min. After the mixture cooling to room temperature, the amount of reducing sugar was determined by DNS method (Miller 1959). In details, 200 µL of reaction solution was added into 300 µL DNS solution and boiled for 10 min. After cooled on ice for 5 min, the mixture was diluted with 1 mL of water and centrifuged at 10,000 g for 5 min. The absorbance of supernatant was measured at 540 nm to calculate the amount of reducing sugar. One unit of the enzyme activity (U) was defined as the amount of enzyme required to liberate 1 µmol of reducing sugar per minute. The amount of enzyme was quantified by the Bradford protein assay, using bovine serum albumin (BSA) as a standard (Bradford 1976).

A high-performance liquid chromatography (HPLC) system (Shimadzu LC-20AT, Japan) was used to identify the enzymatic hydrolysis product of SbChiAJ103. Ten microliters of the purified enzyme was incubated in 190 µL of 1.0% colloidal chitin or NCOS (DP 2–6) at 45 °C for various time intervals (0 min, 2 min, 15 min, 30 min, 60 min, and 24 h). The reaction products were then loaded onto a Sugar Pak I column (6.5×300 mm) on an HPLC system at a column temperature of 75 °C. The used mobile phase was 50 mg/L of EDTA calcium disodium solution and pumped at a flow rate of 0.5 mL/min. The amounts of products from NCOS (DP 2–6) were detected to calculate the activity of SbChiAJ103. All experiments were conducted in triplicate.

Preparation of magnetic nanoparticles

The Fe_3O_4 nanoparticles were prepared by a coprecipitation method, according to the previously reported method (Wang et al. 2018). Six milliliters of 25.0% $NH_3 \cdot H_2O$ was added to 100 mL of a mixture containing 0.8 g of $FeCl_2$ and 3.4 g of $FeCl_3 \cdot 6H_2O$ under a nitrogen atmosphere. Then, the mixture was kept violently stirred using an electric stirrer (Shanghai Mei Yingpu, D2004W) with 1000 rpm at 25 °C for 30 min. The nanoparticles (Fe_3O_4) were magnetically separated with a magnet and then washed three times with absolute ethanol and water, respectively.

To keep the synthesized Fe_3O_4 nanoparticles from oxidization, the hydrolysis of TEOS in alkaline solution was adopted to prepare $Fe_3O_4\&SiO_2$ nanoparticles. Twenty-one milliliters of 25.0% $NH_3 \cdot H_2O$ and 3 mL TEOS were added to an anhydrous ethanol suspension of 1 g Fe_3O_4 at 25 °C for 5 h. The nanoparticles ($Fe_3O_4\&SiO_2$) were recovered by magnetic separation, washed with anhydrous ethanol and water for three times, respectively. For the amino functionalization, 3 mL APTES was added to the suspension containing 200 mg of $Fe_3O_4\&SiO_2$. Then, the mixture was successively stirred in the electric stirrer with 1000 rpm at 25 °C for 2 h and 50 °C for 1.5 h. The resultant particles ($Fe_3O_4\&SiO_2$-HN_2) were separated from the mixture using a magnet and washed three times with anhydrous ethanol and water, respectively.

MMA was used as the linker for the functionalization of the magnetic particles. In order to activate the carboxyl group, 10 mL of MMA was first mixed with 50 mL of MES buffer (pH 6.0, 100 mM) containing EDC (10 mg/mL) and NHS (50 mg/mL) at 20 °C and 220 rpm for 3 h. Subsequently, 200 mg of amino-functionalized $Fe_3O_4\&SiO_2$ nanoparticles was added into the mixture and stirred for another 1 h. Then, the demethyl ester was accomplished in a solution with the tetrahydrofuran (THF) to water ratio of 3:1 containing LiOH (12.5 mg/mL) at room temperature. The obtained nanoparticles ($Fe_3O_4\&SiO_2$-COOH) were recovered and washed with anhydrous ethanol and water until the supernatant became neutral. The obtained particles were labeled as magnetic nanoparticles (MNPs-COOH).

Immobilization of SbChiAJ103

Before immobilizing the enzyme, the carboxyl group is activated with MES buffer (pH 6.0, 100 mM) containing EDC (10 mg/mL) and NHS (50 mg/mL). The standard procedure for the immobilization of chitinase was described as follows: 2.0 mg of MNPs was dispersed in 200 μL of Tris–HCl buffer (50 mM, pH 8.0) containing 240 μg of SbChiAJ103. After incubating the mixture at 25 °C for 2 h, the resultant immobilized SbChiAJ103 was labeled as SbChiAJ103@MNPs, collected by magnetic adsorption, and washed with Tris–HCl buffer (50 mM, pH 8.0). The amounts of protein in the original enzyme solution and washed buffer were determined by the Bradford protein assay to calculate the loaded enzyme (mg/g microparticle). The activities of the resultant SbChiAJ103@MNPs were measured at different immobilization times, SbChiAJ103 doses, and incubation temperatures to determine the optimal conditions of immobilization.

Characterization of different magnetic nanoparticles

A transmission electron microscopy (TEM, JEOL JEM-1010, Japan) was used to measure the morphology of the resultant nanoparticles. The functional groups of the nanoparticles were determined by Fourier transform infrared spectroscopy (FTIR, Thermo Scientific Nicolet iS 10). The magnetic property measurements were carried out on a vibrating sample magnetometer (VSM, Meghnatis Daghigh Kavir Co., Kashan, Iran) with the magnetization pulses frequency of 40 Hz, in the range of experimental temperature (25–80 °C).

Enzymatic property measurements

The optimal pH of SbChiAJ103@MNPs was investigated by measuring its activity in buffer solutions with different pH values. The buffers used in these experiments included sodium citrate buffer (50 mM citric acid—sodium citrate, pH 3.0–6.0), sodium phosphate buffer (50 mM Na_2HPO_3—NaH_2PO_3, pH 6.0–8.0), Tris–HCl buffer (50 mM, pH 7.0–9.0), and glycine–NaOH buffer (50 mM, pH 9.0–10.0). Similarly, the optimum temperature was determined by detecting the activities of SbChiAJ103@MNPs in sodium phosphate buffer (50 mM, pH 7.0) at different temperatures. The optimal temperature and pH of free SbChiAJ103 were determined using the same procedures.

The pH stability analysis of SbChiAJ103@MNPs was performed by immersing them in buffers with different pH (50 mM, pH 3.0–10.0) at 4 °C for 72 h. The residual enzyme activities of SbChiAJ103@MNPs were measured at different time intervals to evaluate the pH stability. The thermal stability of SbChiAJ103@MNPs was studied at 30–60 °C and the storage stability was detected at 4 °C. SbChiAJ103@MNPs were incubated at the predefined temperatures before testing the residual enzyme activity at different time intervals.

To investigate the reusability of SbChiAJ103@MNPs, enzyme activity measurements were repeated for ten consecutive cycles. After each activity measurement, SbChiAJ103@MNPs were magnetically separated from the mixture and washed with pH 7.0 sodium phosphate buffer three times. Then, the recovered SbChiAJ103@MNPs was resuspended and added to a fresh substrate solution for the next activity measurement cycle.

In the above assays, the residual activity was defined as the percentage of activity to their initial enzyme activity. All the experiments were carried out in triplicate.

Enzymatic degradation of chitin

Ten microliters of free SbChiAJ103 or SbChiAJ103@MNPs with the same enzymatic activity (0.12 U) was added to 190 μL of sodium phosphate buffer (50 mM, pH 7.0) containing excess colloidal chitin (1.9 mg) to evaluate their capability to degrade chitin. At time intervals of 1 h, the amount of the generated reducing sugar was determined at 6 h and defined as the enzymatic hydrolysis yield in this work. All the tests were conducted at least three times and data are reported as average values with standard deviations.

GenBank accession number

The gene of *SbChiAJ103* was deposited in the GenBank database under the accession number OP828716. This sequence of chitinase came from *Streptomyces bacillaris*

ATCC 15,855 (the accession number of the whole genome CP029378.1), which was sequenced and annotated in NCBI by our lab. The function of this sequence was verified and the enzymatic properties of the chitinase were characterized in the article.

Results

Expression and bioinformatics analysis

A chitinase gene, named *SbChiAJ103*, was cloned. The gene of *SbChiAJ103* consists of 888 bp, encoding a protein containing 296 amino acids with the molecular weight of 31.5 kDa. The isoelectric point of the protein was predicted to be 5.18. The recombinant chitinase SbChiAJ103 with 6×His C-term tags was purified by a Ni–NTA agarose affinity chromatography. The SDS-PAGE measurement of the obtained enzyme showed only a single band, which referred to a molecular weight of 31.5 kDa (Fig. 1a), consistent with the predicted value and similar to the previously reported chitinases (Bai et al. 2021; Kawase et al. 2006; Zhang et al. 2020). According to the result of sequence alignment by DNAMAN software, SbChiAJ103 displayed the highest sequence identity (82.7%) with GH-19 chitinase from *Streptomyces* (WP_003967541.1). Furthermore, GH-19 chitinase can be further divided into 17 subfamilies based on the sequence networks analysis which was guided by taxonomy and substrate specificity (Orlando et al. 2021). Accordingly, phylogenetic analysis was further conducted and SbChiAJ103 was categorized into the fifth subfamily (CHIT 5), as shown in Fig. 1b. Based on the SMART analysis (Fig. S1), SbChiAJ103 consists of a binding domain and a GH19 catalytic domain. The latter played an important role in the catalytic rate and the product types. Thus, the catalytic domain was analyzed by the multiple sequence alignment. As shown in Fig. 1c, the catalytic domain of SbChiAJ103 contained nine highly conserved α-helices, consistent with the previously reported chitinase from *S. griseus* (Kezuka et al. 2006). The conserved amino acid residues, including Glu150, Thr151, Gly153, and Gln191 residues in the chitin-binding sites, were observed, which is consistent with a previous work (Ohnuma et al. 2012). Besides, SbChiAJ103 showed a sequence of 185 YGKGPIQLSWNFNY 198, similar to the unique conserved motif ([FHY]-G-R-G-[AP]-x-Q-[IL]-[ST]-[FHYW]-[HN]-[FY]-NY) of GH19 chitinases (Udaya Prakash et al. 2010). Therefore, SbChiAJ103 was considered a novel chitinase of the GH 19 family.

Enzymatic activity and products analysis

The substrate specificity of purified SbChiAJ103 toward various substrates was investigated (Fig. S5 and Table 1).

The specific activity of the purified SbChiAJ103 was first measured using colloidal chitin as the substrate and defined as 100.0% for comparison. As can be seen from Table 1, SbChiAJ103 displayed the highest specific activity toward $(GlcNAc)_6$, followed by $(GlcNAc)_4$, $(GlcNAc)_5$, and $(GlcNAc)_3$. SbChiAJ103 cannot hydrolyze $(GlcNAc)_2$. The specific activities of SbChiAJ103 toward NCOS (DP 3–6) were higher than that toward colloidal chitin. This could be explained by the better solubility of NCOS, which allows the substrate to easily access to the catalytic site. At the same time, the better accessibility of substrate resulted in the higher affinity of SbChiAJ103 toward corresponding substrate, which was demonstrated by the K_m values of SbChiAJ103 in Table 1. Obviously, SbChiAJ103 exhibited higher affinity toward these NCOS than that of colloidal chitin. It was considered that the insolubility and crystal structure of colloidal chitin hindered their accessibility to enzymes, thus hampering the processes of catalysis. For the same reason, SbChiAJ103 showed the lowest specific activity toward α-chitin among the substrates. Even employing β-chitin as the substrate, the relative activity of SbChiAJ103 was 1.8 times higher than that of α-chitin, due to the loose structure and relatively low crystallinity of β-chitin (Hajji et al. 2014). These results suggested that SbChiAJ103 exhibited a higher substrate specificity toward NCOS (DP 3–6) than colloidal chitin, different from the reported chitinases (Yang et al. 2016a, b). In addition, the V_{max}/K_m value of $(GlcNAc)_6$ was the highest (as shown in Table 1), followed by $(GlcNAc)_4$, which indicated SbChiAJ103 exhibited higher catalytic efficiencies for NCOS with DP of even number. SbChiAJ103 preferred to hydrolyze NCOS with DP of even number than that of odd number, distinct from that of the GH-19 chitinases from *S. alfalfae* (Lv et al. 2021). The substrate preference of SbChiAJ103 was similar to that of the reported chitinase *Tf*Chi18A (Gaber et al. 2016).

The hydrolysis pattern of SbChiAJ103 was studied to explain its preference for NCOS with DP of an even number. The hydrolysis products from NCOS (DP 2–6) and colloidal chitin were identified with the extension of incubation time. As shown in Fig. 2, the smallest units that SbChiAJ103 chitinase can degrade was $(GlcNAc)_3$. SbChiAJ103 could decompose $(GlcNAc)_3$, releasing $(GlcNAc)_2$ and GlcNAc, which is consistent with the reported research results (Lee et al. 2010; Zhang et al. 2021). The hydrolytic products of $(GlcNAc)_4$ by SbChiAJ103 was only $(GlcNAc)_2$, without $(GlcNAc)_3$ and GlcNAc (Fig. 2C). No $(GlcNAc)_4$ was observed in the hydrolytic products of $(GlcNAc)_5$ (Fig. 2D) and the presence of $(GlcNAc)_3$ in the hydrolytic products of $(GlcNAc)_6$ indicated that SbChiAJ103 is a kind of endochitinase with exochitinase activity, similar to the previously reported plant-derived chitinase (Moore et al. 2004). It is the first microbial-derived GH19 chitinase that simultaneously possessed two hydrolysis modes.

Fig. 1 Enzyme purification and bioinformatics analysis of SbChiAJ103. **a** SDS-PAGE analysis of recombinant SbChiAJ103. Lane M, molecular mass marker of proteins; lane 1, the supernatant of broken bacteria without target protein; lane 2, crude enzyme; lane 3, purified enzyme. **b** Phylogenetic analysis based on amino acid sequences of SbChiAJ103 and 17 subfamilies of GH19 chitinases, presented as a neighbor-joining tree with protein accession numbers, enzyme names of organisms, and subtribe. The scale bar indicates the branch length and the bootstrap method was used to test phylogeny with the number of bootstraps 1000. **c** Multiple sequence alignment of SbChiAJ103 and the chitinases from *Streptomyces griseus* (ChiC), *Streptomyces coelicolor* (ChiG), and rye, *Secale cereale*, seeds (RSC-c). The conserved amino acid sites are marked in red triangles, and α stands for α-helices
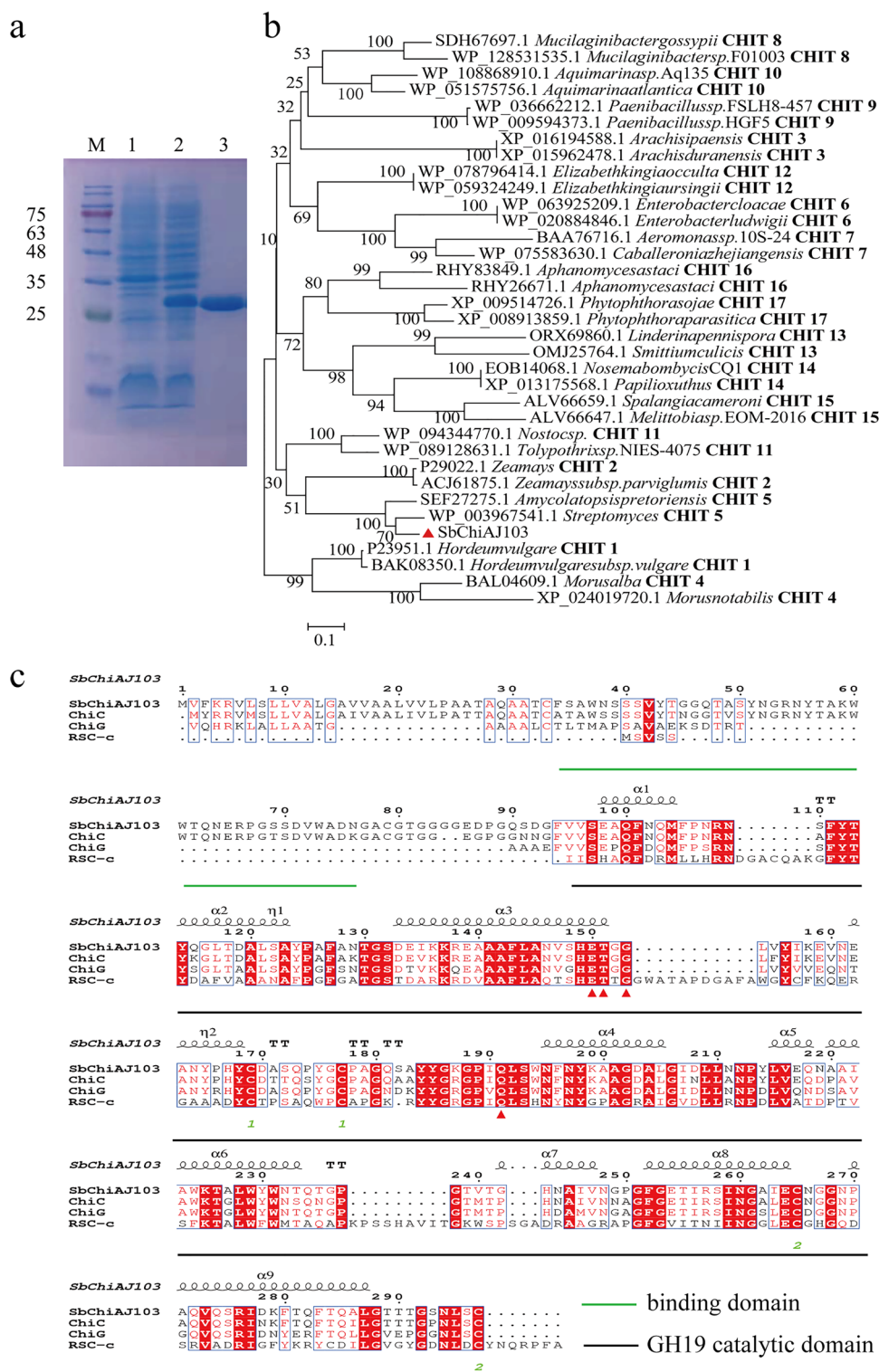
Characterization of immobilized SbChiAJ103

Fe_3O_4&SiO_2 core–shell nanoparticles were synthesized and modified with MMA, for the immobilization of SbChiAJ103 (Fig. 3a). The resultant MMA-modified particle was labeled as MNPs-COOH. TEM experiments were first carried out to characterize the morphologies of original Fe_3O_4 nanoparticles and MNPs-COOH. As shown in Fig. 3b, Fe_3O_4 nanoparticles exhibited a homogeneous spherical structure. After silylation modification and MMA functionalization, the core–shell structure of MNPs-COOH was observed (Fig. 3c). The average

diameters of Fe_3O_4 and MNPs-COOH were calculated to be 5.9 ± 0.7 nm (Fig. S2a) and 11.6 ± 0.8 nm (Fig. S2b), respectively. The modification of particles and subsequent immobilization of SbChiAJ103 were detected by FT-IR analysis (Fig. 3d). In the FT-IR spectra, the peak at 572 cm^{-1} belongs to the absorption peak of Fe–O. The peak at 1091 cm^{-1} is the characteristic peak of Si–O, which emerged after silane modification (Hosseini et al. 2018). The emerging characteristic peak of -COOH at 1402 cm^{-1} confirmed the successful modification of MMA and synthesis of MNPs-COOH (Weber et al. 2000). The peaks at 1534 cm^{-1} and 1465 cm^{-1} could be attributed to the amidic C-N and N–H groups of SbChiAJ103 (Delfino et al. 2013). The presence of these peaks in the spectrum of SbChiAJ103@MNPs proved that SbChiAJ103 was successfully immobilized on MNPs-COOH.

The magnetic properties of Fe_3O_4, MNPs-COOH, and SbChiAJ103@MNPs were measured using a vibrating sample magnetometer at room temperature. No remnant magnetization or coercivity was observed in the magnetization curves (Fig. 3e), indicating that all the particles were paramagnetic. After silane modification and enzyme immobilization, the saturation magnetization values decreased from 64.99 emu/g for Fe_3O_4 to 40.08 emu/g for SbChiAJ103@MNPs due to the integration of silica shell and SbChiAJ103. These values were high enough for the convenient magnetic separation of SbChiAJ103@MNPs (inset in Fig. 3e).

Immobilization studies

The immobilization condition was optimized. Figure 4A shows the effect of immobilization time on the enzyme loading and relative activity of the resultant SbChiAJ103@MNPs. As the immobilization time extended, both the enzyme loading and relative activity of SbChiAJ103@MNPs sharply increased within the initial 1 h, and gradually leveled off thereafter. This result indicated that the functional groups on MNPs could be fully utilized in the first 2 h,

similar to that reported in the literature (Wang et al. 2018). Therefore, 2 h was selected as the optimum immobilization time. The effect of enzyme dose on relative enzyme activity and enzyme loading is shown in Fig. 4B. The enzyme loading increased sharply as the enzyme dose increased from 0 to 120 mg/g MNPs, and almost remained constant thereafter. Meanwhile, the relative enzyme activity also increased first and then decreased slightly, suggesting the existence of an optimum enzyme dose for immobilization. At the optimum enzyme dose (120 mg enzyme/g MNPs), SbChiAJ103@MNPs exhibited the highest relative activity. The steric hindrance induced by the excessive enzyme on the MNPs surface could decrease the accessibility of substrate to the catalytic site and thereby hinder the enzymatic catalysis (Mariño et al. 2021). The immobilization temperature exhibited a slight effect on the enzyme loading and relative enzyme activity of the resultant SbChiAJ103@MNPs (Fig. 4C). The relative enzyme activity and enzyme loading increased with increasing temperature and reached maximums at 25 °C, and then gradually decreased with further increase in temperature. The high immobilization temperature could accelerate the immobilization process. However, high temperatures may also damage the enzyme structure, decreasing the relative activity of SbChiAJ103@MNPs. Thus, the immobilization temperature of 25 °C was used in the following experiments.

At the optimum conditions, SbChiAJ103@MNPs exhibited an enzyme loading of 101.33 mg chitinase/g MNPs with a high relative activity of 3.28 U/mg. This specific enzyme activity is comparable to that of free enzymes, indicating that the long-chain linker MMA used for immobilization has little effect on the mobility and structure of SbChiAJ103.

Biochemical property assays

The optimum reaction conditions (i.e., temperature and pH) of free SbChiAJ103 and SbChiAJ103@MNPs were studied. The optimum pH (sodium phosphate buffer 7.0) of SbChiAJ103@

**Table 1** Substrate specificity of SbChiAJ103

Substrate	Specific activity (U/mg)[a]	Relative activity (%)	K_m (mg/mL)	V_{max} (mM/min)	V_{max}/K_m (μmol/mg/min)
Colloidal chitin	3.5 ± 0.1	100.0 ± 1.4	3.7 ± 0.2	0.4 ± 0.1	0.11
α-chitin	0.7 ± 0.1	19.1 ± 0.1	4.9 ± 0.2	0.2 ± 0.1	0.04
β-chitin	1.2 ± 0.1	33.7 ± 0.6	4.3 ± 0.2	0.3 ± 0.1	0.07
$(GlcNAc)_2$	0.0	0.0	-	-	-
$(GlcNAc)_3$	5.1 ± 0.2	145.7 ± 3.4	3.3 ± 0.2	0.5 ± 0.1	0.15
$(GlcNAc)_4$	11.4 ± 0.1	325.4 ± 1.7	2.0 ± 0.2	0.6 ± 0.1	0.30
$(GlcNAc)_5$	10.1 ± 0.1	289.4 ± 0.9	2.2 ± 0.2	0.6 ± 0.1	0.27
$(GlcNAc)_6$	12.2 ± 0.2	348.0 ± 3.7	1.8 ± 0.2	0.6 ± 0.1	0.33

[a]The activity measurements were determined in sodium phosphate buffer (50 mM, pH 7.0) at 45 °C using 10 mg/mL of corresponding substrate

MNPs were consistent with that of free SbChiAJ103 (Fig. 5a). Moreover, immobilization could stabilize the structure of SbChiAJ103, allowing SbChiAJ103@MNPs to maintain high relative activity under acidic (pH 3.0–5.0) and alkaline (pH 9.0–10.0) conditions (Table S1). The optimum temperatures of both free and immobilized SbChiAJ103 were 45 °C (Fig. 5b). The optimum temperature and pH values of SbChiAJ103 allowed the production of NCOS in a mild condition. Compared with free SbChiAJ103, SbChiAJ103@MNPs exhibited higher relative activity at temperatures above 50 °C. Even at a high temperature of 80 °C, the relative activity of SbChiAJ103@MNPs was still higher than 60.0%. It was considered that the immobilization process prevented SbChiAJ103 from denaturation at a high temperature, resulting in the high relative activity in a wide range of temperatures (50–80 °C) (Table S2).

The pH tolerances and thermal stability of enzymes are essential factors for the enzymatic preparation of NCOS. The pH tolerances of free SbChiAJ103 and SbChiAJ103@MNPs were evaluated by measuring their residual activities after incubation in the solutions with various pH values for different time intervals (Fig. S3). The residual activities of both free and immobilized SbChiAJ103 decreased as the incubation time expanded. The decrease in enzyme activity might be due to the destruction of active sites. However, SbChiAJ103@MNPs displayed higher residual activities than free SbChiAJ103 in the studied range of pH, specifically in acidic (pH 3.0–6.0) and alkaline (pH 9.0–10.0) solutions (Table S3 and Fig. 5c). Even after incubation in pH 10.0 and pH 3.0 for 72 h, SbChiAJ103@MNPs retained more than 70.0% and 30.0% activity, much higher than those of free SbChiAJ103. This result indicated that the immobilization

Fig. 2 HPLC analysis of the enzymatic hydrolysis products catalyzed by SbChiAJ103. Enzymatic hydrolysis products from **A** $(GlcNAc)_2$, **B** $(GlcNAc)_3$, **C** $(GlcNAc)_4$, **D** $(GlcNAc)_5$, **E** $(GlcNAc)_6$, and **F** colloidal chitin. The peaks of standards GlcNAc, $(GlcNAc)_2$, $(GlcNAc)_3$, $(GlcNAc)_4$, $(GlcNAc)_5$, and $(GlcNAc)_6$ are marked as N1, N2, N3, N4, N5, and N6. All reactions were conducted at 45 °C with 1.0% substrate (colloidal chitin or NCOS with DP from 2 to 6) in sodium phosphate buffer (50 mM, pH 7.0)
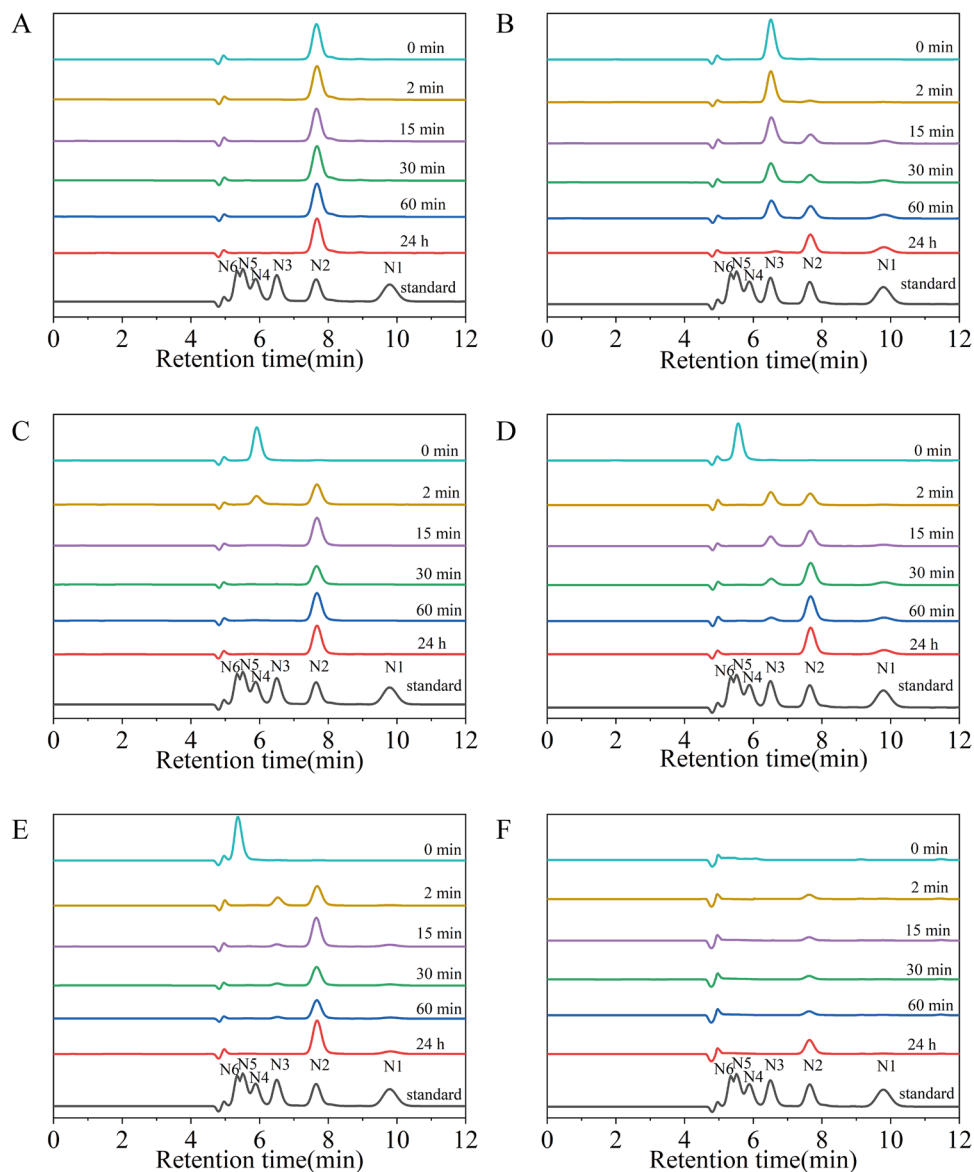
of SbChiAJ103 on MMA-modified MNPs could significantly enhance its pH tolerance. Figure S4 illustrates the thermal stability of free and immobilized SbChiAJ103 at the temperature range of 30–60 °C. In comparison with free SbChiAJ103, SbChiAJ103@MNPs retained higher activities after heating at the studied temperatures (30–60 °C) for 24 h (Table S4 and Fig. 5d). After incubation at 60 °C for 24 h, the residual activity of SbChiAJ103@MNPs was almost twice of free SbChiAJ103, suggesting that the covalent immobilization of SbChiAJ103 enhanced its thermal stability. This finding is consistent with the results demonstrated in other covalent immobilization methods (Prasad and Palanivelu 2014). Additionally, the effect of storage time on the activity of SbChiAJ103@MNPs was also investigated by storing the biocatalysts at 4 °C for 28 days. As shown in Table S5 and Fig. 5e, SbChiAJ103@MNPs could maintain more than 60.0% even stored for 28 days due to the covalent attachment. In contrast, free SbChiAJ103 retained only 40.0% of the initial activity.

The magnetic property of the carrier allows SbChiAJ103@MNPs to be conveniently recovered and reused. The consecutive activity measurements were carried out to evaluate the operational stability of SbChiAJ103@MNPs. As shown in Fig. 5f, after 5 consecutive operations, SbChiAJ103@MNPs could retain more than 85.0% of the initial enzyme activity. Even after 10 recycles, the residual activity of SbChiAJ103@MNPs was maintained at 78.9%, only showing a slightly decrease with the increase of the cycles number (Table S6), because of the possible leakages and denaturation of SbChiAJ103.

Degradation of chitin

Under the optimized reaction conditions, the catalytic performances of free SbChiAJ103 and SbChiAJ103@MNPs were evaluated using colloidal chitin as the substrate. As depicted in Fig. 6, the generated amount of reducing sugar increased sharply within the initial 60 min and tended to saturation thereafter. For the reaction catalyzed by SbChiAJ103@MNPs, the yield of reducing sugar reached 0.68 μmol at 1 h, 1.58 times higher than that by free SbChiAJ103 (0.43 μmol).


Fig. 3 Characterization of MNPs-COOH and SbChiAJ103@MNPs. **a** Schematic diagram illustrating the preparation of SbChiAJ103@MNPs. TEM images of **b** Fe_3O_4 nanoparticles and **c** MNPs-COOH. **d** FTIR spectra of Fe_3O_4, Fe_3O_4&SiO_2, MNPs-COOH, SbChiAJ103@MNPs, and SbChiAJ103. **e** Hysteresis loops of Fe_3O_4, MNPs-COOH and SbChiAJ103@MNPs; Inserted photograph showing the magnetic separation of SbChiAJ103@MNPs
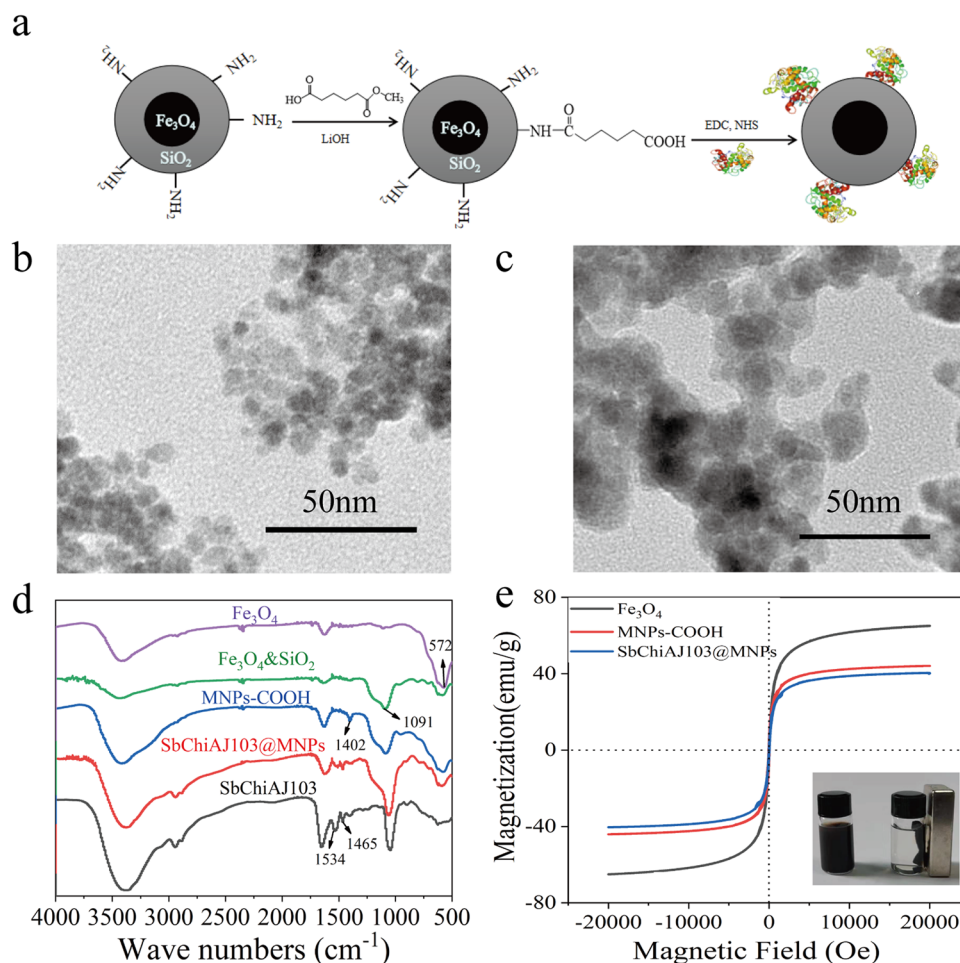
Discussion

GH19 chitinases from S. bacillaris

More than 90% of chitinase in CHIT 5 subfamily were derived from *Actinobacteria* species; only few of them

A

B

C
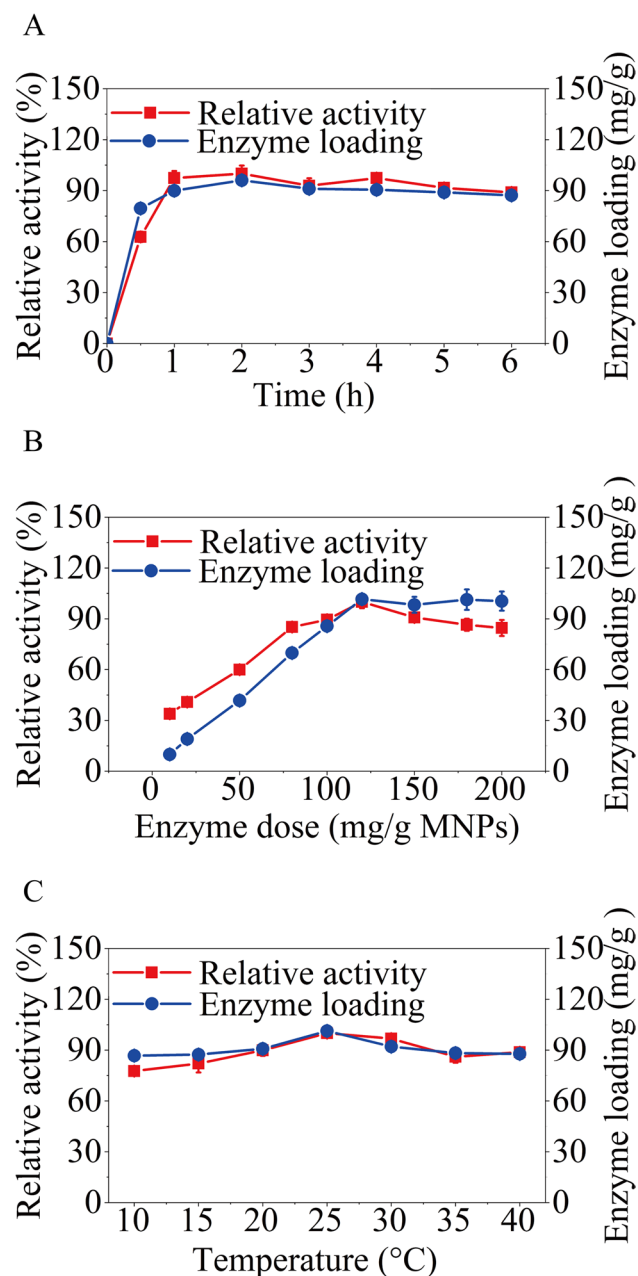
Fig. 4 Optimization of immobilization conditions. Effect of **A** immobilization time, **B** enzyme dose, and **C** immobilization temperatures on enzyme loading and relative activity of resultant SbChiAJ103@MNPs. The values of relative activity were measured using 1.0% w/v colloidal chitin as the substrate in sodium phosphate buffer (50 mM, pH 7.0) at 45 °C. The highest activities of free and immobilized SbChiAJ103 in each figure were respectively defined as 100% for comparison. Enzyme loading was expressed as the amount of chitinase attached to 1 g of MNPs

were derived from *Streptomyces bacillaris* (Orlando et al. 2021). Although these microbial-derived GH19 chitinases were considered to show good antibacterial activity (Hoster et al. 2005; Kawase et al. 2006; Watanabe et al. 1999), few details about the hydrolysis pattern and application in chitin degradation of microbial-derived GH19 chitinases were reported, limiting their wide application in industry. It has been reported that most of the chitinases in CHIT 5 family are "loopless," showing different conserved amino acids compared to that of "loopful" chitinases (Orlando et al. 2021). The different conserved amino acids may lead to the difference in the activity and hydrolysis model of chitinases (Ohnuma et al. 2012). Here, SbChiAJ103 from *S. bacillaris* was considered as a novel microbial-derived GH19 chitinase. In comparison with other GH19 chitinases, SbChiAJ103 shows a different hydrolysis mode. As shown in Fig. 7, it was believed that SbChiAJ103, acting as an exochitinase, could recognize the NCOS chain containing at least three monosaccharide units and release $(GlcNAc)_2$. The exochitinase activity of SbChiAJ103 determined that $(GlcNAc)_2$ was the main enzymatic hydrolysis product, regardless of which NCOS was used as the substrate. On the other hand, the presence of $(GlcNAc)_3$ in the enzymatic hydrolysis products from $(GlcNAc)_6$ suggested that SbChiAJ103 could exhibit endochitinase activity. It was speculated that SbChiAJ103 could bind the NCOS chain containing more than four monosaccharide units and cut at the middle of the four bound monosaccharides. Consequently, $(GlcNAc)_3$ emerged as an intermediate product when $(GlcNAc)_6$ was used as the substrate, as shown in Fig. 2E. Therefore, SbChiAJ103 was considered as the first reported microbial-derived GH19 chitinase that simultaneously exhibited endochitinase and exochitinase activity, according to the enzymatic hydrolysis results of NCOS (Fig. 2 and Fig. 7).

Although the smallest recognition unit was $(GlcNAc)_3$, SbChiAJ103 was more inclined to hydrolyze $(GlcNAc)_4$ (Table 1). The K_m value toward $(GlcNAc)_4$ is less than that of $(GlcNAc)_3$, indicating the higher affinity between SbChiAJ103 and $(GlcNAc)_4$. It was speculated that $(GlcNAc)_4$ could exactly fit the binding pocket of SbChiAJ103, while $(GlcNAc)_3$ was too short to tightly bind to SbChiAJ103, resulting in the preference of SbChiAJ103 to $(GlcNAc)_4$ and the high degradation rate of $(GlcNAc)_4$. Similarly, the substrate affinity of SbChiAJ103 toward $(GlcNAc)_6$ was higher than that of $(GlcNAc)_5$ (Table 1), as half of the products from $(GlcNAc)_5$ was $(GlcNAc)_3$. This point could also explain the preference of SbChiAJ103 to NCOS with even DP (Fig. 2), because $(GlcNAc)_3$ that cannot bind tightly to SbChiAJ103 always appeared as an intermedia in the degradation of NCOS with odd DP. Overall, SbChiAJ103 was considered as a novel member

of GH19 chitinases with a preference for NCOS with even DP (Table 1).

SbChiAJ103 showed an optimum pH of 7.0 and an optimum temperature of 45 °C. At a relatively low temperature (< 50 °C), its enzyme activity was higher than SaChiB (2.40 U/mg) from *Streptomyces alfalfae* and ChiIS (1.80 U/mg) from *Streptomyces griseus* (Lv et al. 2021; Hoster et al. 2005). This could be helpful to avoid the requirement of high temperature and reduce the cost. Furthermore, the optimum pH of SbChiAJ103 was neutral, different from the acidic optimum pH of others (Mohammadzadeh et al. 2017; Prasad and Palanivelu 2014; Sousa et al. 2019). This property could avoid the usage of acidic agent in

the production of NCOS. Overall, SbChiAJ103 exhibited a high enzymatic activity at a mild condition (45 °C, pH 7.0), which possessed the potential in the industrial production of NCOS.

Improved immobilization of SbChiAJ103

Fe_3O_4-SiO_2 MNPs functionalized with mono-methyl adipate were used as the carriers to immobilize SbChiAJ103. The long linker allowed the immobilized SbChiAJ103 to maintain a high specific activity (3.28 U/mg), comparable to that of free SbChiAJ103. Moreover, due to the high specific area and efficient covalent cross-linking,

Fig. 5 Studies on optimal reactions condition, stability, and reusability. Effect of **a** pH and **b** temperature on the activities of free and immobilized SbChiAJ103. The blue lines indicate SbChiAJ103@MNPs, and the red lines indicate SbChiAJ103. The highest activity of free SbChiAJ103 was defined as 100% for comparison. **c** pH tolerance, **d** temperature stability, **e** storage stability, and **f** reusability of SbChiAJ103@MNPs. For **c**, pH 3.0–5.0: sodium citrate buffer; pH 6.0–7.0: sodium phosphate buffer; pH 8.0: Tris–HCl buffer; pH 9.0–10.0: Glycine–NaOH buffer. All the reactions were done with 1.0% w/v colloidal chitin as the substrate, and the activities (**c**–**f**) were measured at 45 °C in sodium phosphate buffer (50 mM, pH 7.0). The initial activities of free and immobilized SbChiAJ103 (**c**–**f**) were respectively defined as 100% for calculating the relative activities. The statistical analyses were conducted by a Tukey test for statistical comparison. *p-value < 0.05 (significant difference); **p-value < 0.01 (highly significant difference)
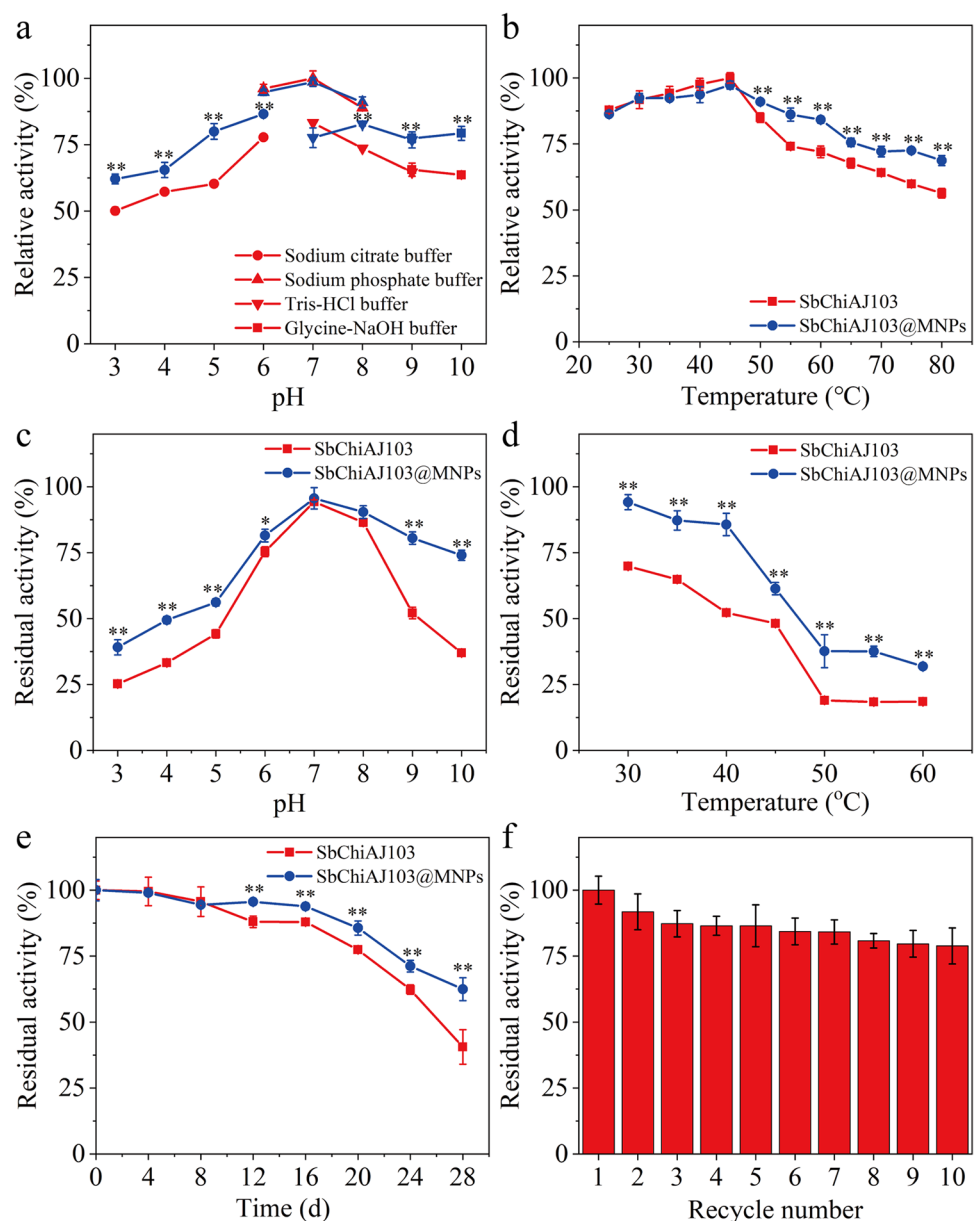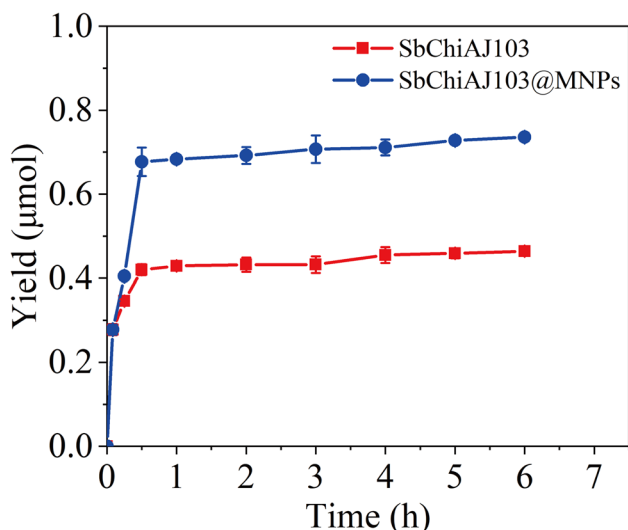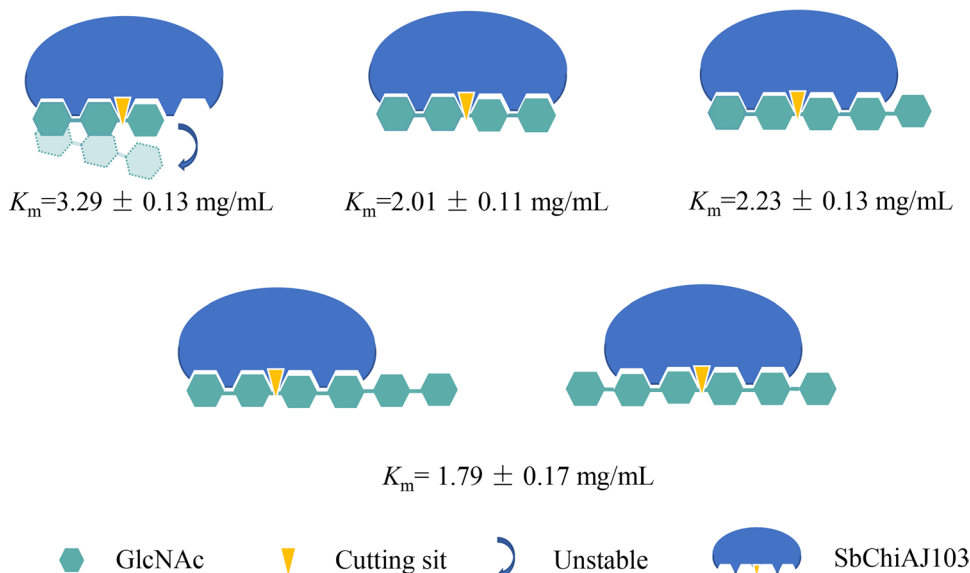
Fig. 6 Time courses of the amounts of enzymatic hydrolysis products catalyzed by free and immobilized SbChiAJ103. Ten microliters of free ChiAJ103 and SbChiAJ103@MNPs with the same enzymatic activity (0.12 U) was added to 190 µL of sodium phosphate buffer (50 mM, pH 7.0) containing excess colloidal chitin (1.9 mg) at 45 °C in these processes

the enzyme loading in this work (101.33 mg/g) is much higher than that of the previously reported immobilized chitinase, whose enzyme loadings were 6.20 mg/g (Kidibule et al. 2021) and 25.10 mg/g (Wang et al. 2018), respectively. The high enzyme loading combined with the high specific activity of SbChiAJ103@MNPs holds the promise for the high-efficiency production of NCOS.

Even after incubation at 45 °C for 24 h, SbChiAJ103@ MNPs could maintain more than 60.0% initial activity (Fig. 5d), showing excellent pH and temperature stabilities. After being recycled 10 times, SbChiAJ103@MNPs could retain almost 78.9% of the initial activity (Fig. 5f). The recycling performance of SbChiAJ103@MNPs was better than that of the reported immobilized chitinase (52.1% residual activity after 6 usage cycles) fixed by the dialdehyde cellulose linker (Guo et al. 2021). By virtue of the improved pH, temperature, and storage stability, as well as the outstanding reusability, SbChiAJ103@ MNPs exhibited superior performance in the degradation of colloidal chitin (Fig. 5). The immobilized SbChiAJ103 with the stabilized structure could maintain high enzymatic hydrolysis yield during the degradation process (Fig. 6). SbChiAJ103@MNPs exhibited a $(GlcNAc)_2$ yield of 0.68 µmol at 1 h, 1.58 times higher than that by free SbChiAJ103. It was considered that the immobilization of SbChiAJ103 stabilized the enzyme structure and lead to more enzymatic hydrolysis products.

In conclusion, a GH19 endochitinase with exochitinase activity from *Streptomyces bacillaris*, SbChiAJ103, was first characterized and immobilized with mono-methyl adipate as the linker. The immobilization process significantly improved the pH tolerance, thermal stability, and storage stability of SbChiAJ103. Furthermore, the immobilized SbChiAJ103 could be conveniently recovered and reused by magnetic separation. Combining the neutral optimum pH, the immobilized SbChiAJ103 reported in this work may pave the way to the large-scale production of $(GlcNAc)_2$.

Fig. 7 Schematic diagram of hydrolysis mode of SbChiAJ103

$K_m=3.29 \pm 0.13$ mg/mL

$K_m=2.01 \pm 0.11$ mg/mL

$K_m=2.23 \pm 0.13$ mg/mL

$K_m= 1.79 \pm 0.17$ mg/mL

GlcNAc   Cutting sit   Unstable   SbChiAJ103

Data availability All data generated or analyzed during this study are included in this published article and its supplementary information files.

Declarations

Conflict of interest The authors declare no competing interests.

References

Bai L, Kim J, Son K, Chung C, Shin D, Ku B, Kim D, Park H (2021) Novel bi-modular GH19 chitinase with broad pH stability from a fibrolytic intestinal symbiont of *Eiseniafetida*, *Cellulosimicrobiumfunkei* HY-13. Biomolecules 11:1735. https://doi.org/10.3390/biom11111735

Barbosa O, Ortiz C, Berenguer-Murcia A, Torres R, Rodrigues RC, Fernandez-Lafuente R (2014) Glutaraldehyde in bio-catalysts design: a useful crosslinker and a versatile tool in enzyme immobilization. Rsc Adv 4:1583–1600. https://doi.org/10.1039/c3ra45991h

Bradford MM (1976) A rapid and sensitive method for the quantitation quantities microgram principle of protein-dye binding. Anal Biochem 72:248–254. https://doi.org/10.1016/0003-2697(76)90527-3

Cantarel BL, Coutinho PM, Rancurel C, Bernard T, Lombard V, Henrissat B (2009) The Carbohydrate-Active EnZymes database (CAZy): an expert resource for Glycogenomics. Nucleic Acids Res 37:D233–D238. https://doi.org/10.1093/nar/gkn663

Chen J, Shen C, Liu C (2010) N-Acetylglucosamine: production and applications. Mar Drugs 8:2493–2516. https://doi.org/10.3390/md8092493

Chen W, Jiang X, Yang Q (2020) Glycoside hydrolase family 18 chitinases: the known and the unknown. Biotechnol Adv 43:107553. https://doi.org/10.1016/j.biotechadv.2020.107553

Delfino I, Portaccio M, Ventura BD, Mita DG, Lepore M (2013) Enzyme distribution and secondary structure of sol–gel immobilized glucose oxidase by micro-attenuated total reflection FT-IR spectroscopy. Mater Sci Eng, C 33:304–310. https://doi.org/10.1016/j.msec.2012.08.044

Doan CT, Tran TN, Wang S (2021) Production of thermophilic chitinase by *Paenibacillus sp.* TKU052 by bioprocessing of chitinous fishery wastes and its application in N-acetyl-d-glucosamine production. Polymers-Basel 13:3048. https://doi.org/10.3390/polym13183048

Ein Ali Afjeh M, Pourahmad R, Akbari-Adergani B, Azin M (2020) Characteristics of glucose oxidase immobilized on magnetic chitosan nanoparticles. Food Sci Tech-Brazil 40:68–75. https://doi.org/10.1590/fst.32618

Fujita K, Shimomura K, Yamamoto K, Yamashita T, Suzuki K (2006) A chitinase structurally related to the glycoside hydrolase family 48 is indispensable for the hormonally induced diapause termination in a beetle. Biochem Bioph Res Co 345(1):502–507. https://doi.org/10.1016/j.bbrc.2006.04.126

Gaber Y, Mekasha S, Vaaje-Kolstad G, Eijsink VGH, Fraaije MW (2016) Characterization of a chitinase from the cellulolytic actinomycete *Thermobifidafusca*. Biochim et Biophys Acta (BBA) - Proteins Proteomics 1864:1253–1259. https://doi.org/10.1016/j.bbapap.2016.04.010

Gao L, Sun J, Secundo F, Gao X, Xue C, Mao X (2018) Cloning, characterization and substrate degradation mode of a novel chitinase from *Streptomyces albolongus* ATCC 27414. Food Chem 261:329–336. https://doi.org/10.1016/j.foodchem.2018.04.068

Guo H, Lei B, Yu J, Chen Y, Qian J (2021) Immobilization of lipase by dialdehyde cellulose crosslinked magnetic nanoparticles. Int J Biol Macromol 185:287–296. https://doi.org/10.1016/j.ijbiomac.2021.06.073

Hajji S, Younes I, Ghorbel-Bellaaj O, Hajji R, Rinaudo M, Nasri M, Jellouli K (2014) Structural differences between chitin and chitosan extracted from three different marine sources. Int J Biol Macromol 65:298–306. https://doi.org/10.1016/j.ijbiomac.2014.01.045

Hoell IA, Dalhus B, Heggset EB, Aspmo SI, Eijsink VGH (2006) Crystal structure and enzymatic properties of a bacterial family 19 chitinase reveal differences from plant enzymes. FEBS J 273:4889–4900. https://doi.org/10.1111/j.1742-4658.2006.05487.x

Hosseini SH, Hosseini SA, Zohreh N, Yaghoubi M, Pourjavadi A (2018) Covalent immobilization of cellulase using magnetic poly(ionic liquid) support: improvement of the enzyme activity and stability. J Agr Food Chem 66:789–798. https://doi.org/10.1021/acs.jafc.7b03922

Hoster F, Schmitz JE, Daniel R (2005) Enrichment of chitinolytic microorganisms: isolation and characterization of a chitinase exhibiting antifungal activity against phytopathogenic fungi from a novel *Streptomyces* strain. Appl Microbiol Biot 66:434–442. https://doi.org/10.1007/s00253-004-1664-9

Jeffrey Yuan AAJB (1999) Multiclustal_ a systematic method for surveying ClustalW alignment parameters. Bioinformatics 15(10):862–863. https://doi.org/10.1093/bioinformatics/15.10.862

Kawase TNUJ, Yokokawa S, Saito A, Fujii T, Nikaidou N, Miyashita K, Watanabe T (2006) Comparison of enzymatic and antifungal properties between family 18 and 19 chitinases from *S. coelicolor* A3(2). Biosci Biotechnol Biochem 70:988–998. https://doi.org/10.1271/bbb.70.988

Kezuka Y, Ohishi M, Itoh Y, Watanabe J, Mitsutomi M, Watanabe T, Nonaka T (2006) Structural studies of a two-domain chitinase from *Streptomyces griseus* HUT6037. J Mol Biol 358:472–484. https://doi.org/10.1016/j.jmb.2006.02.013

Kidibule PE, Costa J, Atrei A, Plou FJ, Fernandez-Lobato M, Pogni R (2021) Production and characterization of chitooligosaccharides by the fungal chitinase Chit42 immobilized on magnetic nanoparticles and chitosan beads: selectivity, specificity and improved operational utility. Rsc Adv 11:5529–5536. https://doi.org/10.1039/d0ra10409d

Lee SG, Koh HY, Han SJ, Park H, Na DC, Kim I, Lee HK, Yim JH (2010) Expression of recombinant endochitinase from the Antarctic bacterium, *Sanguibacterantarcticus* KOPRI 21702 in Pichia pastoris by codon optimization. Protein Expres Purif 71:108–114. https://doi.org/10.1016/j.pep.2010.01.017

Lei L, Liu X, Li Y, Cui Y, Yang Y, Qin G (2011) Study on synthesis of poly(GMA)-grafted Fe_3O_4/SiO_X magnetic nanoparticles using atom transfer radical polymerization and their application for lipase immobilization. Mater Chem Phys 125:866–871. https://doi.org/10.1016/j.matchemphys.2010.09.031

Lv C, Gu T, Ma R, Yao W, Huang Y, Gu J, Zhao G (2021) Biochemical characterization of a GH19 chitinase from *Streptomyces alfalfae* and its applications in crystalline chitin conversion and biocontrol. Int J Biol Macromol 167:193–201. https://doi.org/10.1016/j.ijbiomac.2020.11.178

Mao X, Guo N, Sun J, Xue C (2017) Comprehensive utilization of shrimp waste based on biotechnological methods: a review. J Clean Prod 143:814–823. https://doi.org/10.1016/j.jclepro.2016.12.042

Mariño MA, Moretti P, Tasic L (2021) Immobilized commercial cellulases onto amino-functionalized magnetic beads for biomass hydrolysis: enhanced stability by non-polar silanization. Biomass Convers Bior, pp 1–11. https://doi.org/10.1007/s13399-021-01798-y

Miller GL (1959) Use of dinitrosaIicyIic acid reagent for determination of reducing sugar. Anal Chem 31:426–428. https://doi.org/10.1021/ac60147a030/

Mohammadzadeh R, Agheshlouie M, Mandavinia GR (2017) Expression of chitinase gene in BL21 pET system and investigating the biocatalystic performance of chitinase-loaded AlgSep nanocomposite beads. Int J Biol Macromol 104:1664–1671. https://doi.org/10.1016/j.ijbiomac.2017.03.119

Moore KG, Price MS, Boston RS, Weissinger AK, Payne GA (2004) A chitinase from Tex6 maize kernels inhibits growth of Aspergillus flavus. Phytopathology 94:82–87. https://doi.org/10.1094/PHYTO.2004.94.1.82

Mukherjee G, Sen SK (2006) Purification, characterization, and antifungal activity of chitinase from *Streptomyces venezuelae* P10. Curr Microbiol 53:265–269. https://doi.org/10.1007/s00284-005-0412-4

Ngo D, Kim M, Kim S (2008) Chitin oligosaccharides inhibit oxidative stress in live cells. Carbohyd Polym 74:228–234. https://doi.org/10.1016/j.carbpol.2008.02.005

Nishitani Y, Horiuchi A, Aslam M, Kanai T, Atomi H, Miki K (2018) Crystal structures of an archaeal chitinase ChiD and its ligand complexes. Glycobiology 28:418–426. https://doi.org/10.1093/glycob/cwy024

Ohnuma T, Numata T, Osawa T, Inanaga H, Okazaki Y, Shinya S, Kondo K, Fukuda T, Fukamizo T (2012) Crystal structure and chitin oligosaccharide-binding mode of a 'loopful' family GH19 chitinase from rye, *Secalecereale*, seeds. FEBS J 279(19):3639–3651. https://doi.org/10.1111/j.1742-4658.2012.08723.x

Orlando M, Buchholz PCF, Lotti M, Pleiss J (2021) The GH19 Engineering Database: sequence diversity, substrate scope, and evolution in glycoside hydrolase family 19. Plos One 16(10):e256817. https://doi.org/10.1371/journal.pone.0256817

Prasad M, Palanivelu P (2014) A novel method for the immobilization of a thermostable fungal chitinase and the properties of the immobilized enzyme. Biotechnol Appl Bioc 61:441–445. https://doi.org/10.1002/bab.1179

Ricardi NC, Arenas LT, Benvenutti EV, Hinrichs R, Flores EEE, Hertz PF, Costa TMH (2021) High performance biocatalyst based on β-d-galactosidase immobilized on mesoporous silica/titania/chitosan material. Food Chem 359:129890. https://doi.org/10.1016/j.foodchem.2021.129890

Schultz J, Copley RR, Doerks T, Ponting CP, Bork P (2000) SMART: a web-based tool for the study of genetically mobile domains. Nucleic Acids Res 28(1):231–234. https://doi.org/10.1093/nar/28.1.231

Sousa AJS, Silva CFB, Sousa JS, Monteiro Junior JE, Freire JEC, Sousa BL, Lobo MDP, Monteiro-Moreira ACO, Grangeiro TB (2019) A thermostable chitinase from the antagonistic *Chromobacteriumviolaceum* that inhibits the development of phytopathogenic fungi. Enzyme Microb Tech 126:50–61. https://doi.org/10.1016/j.enzmictec.2019.03.009

Tamura K, Stecher G, Peterson D, Filipski A, Kumar S (2013) MEGA6: molecular evolutionary genetics analysis version 6.0. Mol Biol Evol 30(12):2725–2729. https://doi.org/10.1093/molbev/mst197

Udaya Prakash NA, Jayanthi M, Sabarinathan R, Kangueane P, Mathew L, Sekar K (2010) Evolution, homology conservation, and identification of unique sequence signatures in GH19 family chitinases. J Mol Evol 70:466–478. https://doi.org/10.1007/s00239-010-9345-z

Wang M, Qi W, Su R, He Z (2015) Advances in carrier-bound and carrier-free immobilized nanobiocatalysts. Chem Eng Sci 135:21–32. https://doi.org/10.1016/j.ces.2015.03.051

Wang W, Guo N, Huang W, Zhang Z, Mao X (2018) Immobilization of chitosanases onto magnetic nanoparticles to enhance enzyme performance. Catalysts 8:401. https://doi.org/10.3390/catal8090401

Watanabe T, Kanai R, Kawase T, Tanabe T, Mitsutomi M, Sakuda S, Miyashita K (1999) Family 19 chitinases of *Streptomyces* species: characterization and distribution. Microbiology (society for General Microbiology) 145:3353–3363. https://doi.org/10.1099/00221287-145-12-3353

Weber A, Tesch S, Thomas B, Schmiers H (2000) New ways of determining structural groups in brown coals and their bioconversion products by FTIR spectroscopy. Appl Microbiol Biotechnol 54:681–685. https://doi.org/10.1007/s002530000419

Yang S, Fu X, Yan Q, Guo Y, Liu Z, Jiang Z (2016) Cloning, expression, purification and application of a novel chitinase from a thermophilic marine bacterium *Paenibacillusbarengoltzii*. Food Chem 192:1041–1048. https://doi.org/10.1016/j.foodchem.2015.07.092

Yang S, Fu X, Yan Q, Jiang Z, Wang J (2016) Biochemical characterization of a novel acidic exochitinase from *Rhizomucormiehei* with antifungal activity. J Agr Food Chem 64:461–469. https://doi.org/10.1016/j.foodchem.2015.07.092

Yano S, Honda A, Rattanakit N, Noda Y, Wakayama M, Plikomol A, Tachiki T (2008) Cloning and expression of chitinase a gene from *Streptomyces cyaneus* SP-27: the enzyme participates in protoplast formation of *Schizophyllum commune*. Biosci Biotechnol Biochem 72:1853–1859. https://doi.org/10.1271/bbb.80110

Zhang W, Liu Y, Ma J, Yan Q, Jiang Z, Yang S (2020) Biochemical characterization of a bifunctional chitinase/lysozyme from *Streptomyces sampsonii* suitable for N-acetyl chitobiose production. Biotechnol Lett 42:1489–1499. https://doi.org/10.1007/s10529-020-02834-z

Zhang W, Ma J, Yan Q, Jiang Z, Yang S (2021) Biochemical characterization of a novel acidic chitinase with antifungal activity from *Paenibacillusxylanexedens* Z2–4. Int J Biol Macromol 182:1528–1536. https://doi.org/10.1016/j.ijbiomac.2021.05.111

Zheng C, Ding K, Huang X, Yang L, Lei Y, Wang Y (2022) A bioprosthetic heart valve prepared by copolymerization of 2-isocyanatoethyl methacrylate modified pericardium and functional monomer. Compos Part B: Eng 238:109922. https://doi.org/10.1016/j.compositesb.2022.109922